



CHORUS

This is the accepted manuscript made available via CHORUS. The article has been published as:

Branching and Fragmentation of Dipole Strength in ^{181}Ta in the Region of the Scissors Mode

C. T. Angell, R. Hajima, T. Shizuma, B. Ludewigt, and B. J. Quiter

Phys. Rev. Lett. **117**, 142501 — Published 26 September 2016

DOI: [10.1103/PhysRevLett.117.142501](https://doi.org/10.1103/PhysRevLett.117.142501)

Branching and fragmentation of dipole strength in ^{181}Ta in the region of the scissors mode

C. T. Angell,* R. Hajima, and T. Shizuma

Quantum Beam Science Center, Japan Atomic Energy Agency, Tokai-mura, Ibaraki 319-1184, Japan[†]

B. Ludewigt and B. J. Quiter

Lawrence Berkeley National Laboratory, Berkeley, California 94720, USA

(Dated: August 3, 2016)

Abstract

In recent measurements of the scissors mode in radiative decay experiments, transition strengths were observed that were double that expected from theory and systematics well established from measurements on the radiative excitation channel, that is, using nuclear resonance fluorescence (NRF). Additional strength as measured with NRF can only be present as heretofore unobserved branching or fragmentation of the scissors mode. Such possibilities were investigated in a transmission NRF measurement on the deformed, odd-mass ^{181}Ta , using a quasi-monoenergetic γ -ray beam at two beam energies. This measurement further influences applications using transmission NRF to assay or detect odd-mass fissile isotopes. A large branching, $\approx 75\%$, of small resonances to excited states was discovered. In contrast, previous studies using NRF of the scissors-mode strength in odd-mass nuclei assumed no branching existed. The presently observed branching, combined with the observed highly-fragmented elastic strength, could reconcile the scissors-mode strength observed in NRF measurements with the expectations for enhanced scissors-mode strength from radiative decay experiments.

PACS numbers: 21.10.Re, 25.20.Dc, 27.70.+q

Keywords: self-absorption, nuclear resonance fluorescence, scissors mode, ^{181}Ta

The scissors mode is a collective, orbital $M1$ excitation found in virtually all deformed atomic nuclei, and is considered an oscillation of the protons against the neutrons in a scissors-like fashion, and may be a universal phenomenon in deformed quantum systems [1–3]. Manifested as a set of discrete resonances at 2–3 MeV in high-resolution nuclear resonance fluorescence (NRF) experiments, it has been extensively studied exhibiting regular behavior that varies smoothly between neighboring nuclei with the experimentally established systematics for the sum strength in proportion to deformation and in substantial agreement with theoretical calculations and sum-rule predictions [4]. Odd-mass nuclei, having the scissors-mode strength highly fragmented, are thought to have up to 2/3 the expected scissors-mode strength in resonances not directly resolvable [5].

Recently, however, in a measurement probing the radiative-decay channel, where decay γ -rays were measured following excitation of the nucleus by light ion-scattering, double the expected scissors-mode strength was observed in both even and odd-mass actinide nuclei compared to expectations established for the radiative excitation channel, that is, using NRF [6]. The same phenomenon of increased strength was observed a decade prior in lanthanide nuclei using similar measurements of radiative decay following neutron capture [7, 8] and ($^3\text{He}, \alpha$) scattering [8], which observation has been reinforced in a contemporary measurement using (p, d) scattering [9]. This discrepancy in measured strength between the radiative excitation and radiative decay channels for the scissors mode remains its greatest mystery.

Additional scissors-mode strength can only be present in the radiative excitation channel if it were to occur as heretofore unobserved fragmentation or branching, forbearing the alternative that the additional strength is confined solely to the radiative decay channel. This alternative could happen if states excited by ion-scattering at energies up to 10 MeV de-excite emitting 2-3 MeV γ -rays more strongly than would be expected from the ground state scissors-mode strength (see e.g. Krtička *et al.* [7]). Nevertheless, the possibility of strong branching of the scissors mode to excited states was recently suggested from theoretical calculations [10]. To date, such branching of the scissors mode has not been investigated, and it was assumed by necessity to be negligible in previous attempts with NRF to investigate the total strength and fragmentation of the scissors mode in odd-mass nuclei [5]. The observation of additional scissors-mode strength using NRF, as branching or fragmentation, would not only challenge theoretical models of the scissors mode, but also impact proposed applications to use the NRF of scissors-mode resonances for detection or assay of odd-mass fissile nuclei [11, 12].

In this letter, we demonstrate the presence of a large branching of resonances at the energy of the scissors mode to excited states and verify the high fragmentation of strength in odd-mass nuclei by measuring the transmission NRF of ^{181}Ta using a quasi-monoenergetic γ -ray beam, which provides enhanced sensitivity compared with traditional measurements using a bremsstrahlung source. ^{181}Ta was chosen because it has a strong resonance at 2.3 MeV [13] enabling the accuracy of the self-absorption measurement to be verified.

Transmission NRF [14] is a well established technique that combines NRF with a self-absorption measurement [15] to determine both the elastic scattering strength and the total strength, and from the two, the ground state branching ratio. In NRF, the de-excitation of dipole states is measured after their exci-

tation by a γ -ray beam yielding a signal strength proportional to the elastic-scattering strength, which is the absorption (ground-state) integrated cross section times the ground state branching ratio, $b_0 I_{cs}$. The self-absorption aspect is obtained by placing a sample consisting of the same isotope upstream. NRF in the upstream (absorption) target causes a decrease in NRF scattering in the downstream (witness) target. That decrease is measured as an absorption ratio, R , being one minus the ratio of the observed ground state integrated cross section with (\dagger) and without the absorption target:

$$R(I_{cs}) = 1 - \frac{b_0 I_{cs}^\dagger}{b_0 I_{cs}}. \quad (1)$$

R (for a fixed absorption target thickness) is proportional to the total absorption integrated cross section, I_{cs} (see Metzger [15] for derivation).

Because of the highly fragmented strength in odd-mass nuclei, the transmission NRF method was extended to determine the average absorption properties of multiple resonances. While individual elastic integrated cross sections, $b_0 I_{cs}$, may be obtained from the NRF spectrum, sensitivity may be too low to determine I_{cs} from the self-absorption measurement for each resonance separately. I_{cs} can, instead, be determined in aggregate. A measure of the combined scattering strength of multiple resonances is provided in the average elastic scattering cross section, $\langle \sigma_{\gamma\gamma} \rangle$:

$$\langle \sigma_{\gamma\gamma} \rangle = \rho \langle b_0 I_{cs} \rangle, \quad (2)$$

where ρ is the level density and $\langle b_0 I_{cs} \rangle$ is the average of $b_0 I_{cs}$ in a given energy region (brackets are used throughout to indicate average quantities). R for many resonances is then:

$$R(\langle I_{cs} \rangle^*) = 1 - \frac{\langle \sigma_{\gamma\gamma}^\dagger \rangle}{\langle \sigma_{\gamma\gamma} \rangle} \quad (3)$$

and is proportional to the weighted average of I_{cs} , defined here as $\langle I_{cs} \rangle^*$. The weighting for $\langle I_{cs} \rangle^*$ is approximately by I_{cs} because resonances both absorb and scatter radiation proportional to I_{cs} so that I_{cs} gets effectively counted twice and may be skewed slightly if $\langle \sigma_{\gamma\gamma} \rangle$ includes branching to excited states. The relationship between R and $\langle I_{cs} \rangle^*$ was determined using numerical calculations of absorption for a *single* Doppler-broadened resonance (see Eq. 4 in Ref. [14] [16] and, for further discussion, Ref. [15]). This avoids needing to assume a specific distribution for I_{cs} , but requires appropriately weighting quantities derived from the scattering spectrum when used jointly with $\langle I_{cs} \rangle^*$. Thus, similarly to how $\langle I_{cs} \rangle^*$ is naturally weighted, we define a weighted average of $b_0 I_{cs}$ that also takes into account possible skewing due to the inclusion of branching to the first excited state at 6 keV (b_1) as (summation index implied over all resonances in a given region):

$$\langle b_0 I_{cs} \rangle^* = \frac{\sum (b_0 I_{cs})(b_0 + b_1) I_{cs}}{\sum (b_0 + b_1) I_{cs}}. \quad (4)$$

$\langle b_0 \rangle$, the average ground state branching ratio, is then:

$$\langle b_0 \rangle = \frac{\langle b_0 I_{cs} \rangle^*}{\langle I_{cs} \rangle^*}. \quad (5)$$

These equations assume that b_0 varies stochastically such that weighting by $b_0 I_{cs}$ is equivalent to weighting by I_{cs} .

The average resonance properties, as defined above, were measured using transmission NRF at two nominal beam energies, $E_\gamma = 2.28$ and 2.75 MeV. The average was taken of both $M1$ and $E1$ resonances since the transition multipolarity could not be determined. Natural metallic Ta (99.988% ^{181}Ta) targets were used; the scattering target was 0.74 cm thick. At $E_\gamma = 2.28$ MeV, two unique data sets were obtained: the ratio of a Ta absorber (2 cm-thick) to no absorber, and of a Ta absorber (2 cm, separate measurement) to a Pb absorber (2.6 cm). For the second set, the beam energy was shifted down by 10 keV ($E_\gamma = 2.27$ MeV). The Pb absorber measurement was done to verify that the present absorption signature was due entirely to resonant absorption in Ta. The absorption ratios agreed. At $E_\gamma = 2.75$ MeV, one data set was obtained: the ratio of a Ta absorber (3 cm) to no absorber.

These measurements were done substantially similar to our previous transmission NRF experiment on ^{27}Al [14], using the same quasi-monoenergetic γ -ray beam at the HI γ S facility in Durham, NC, USA [17], the same experimental setup, the same analysis techniques, and the same procedure for accounting for systematic uncertainties (due to determining the beam energy profile, flux, and pileup), with the following extension: the background was subtracted componentwise in order to obtain the total resonance strength in spite of it being highly fragmented.

The background consisted of four main components, in order of subtraction: pileup of counts, room background, small-angle Compton scattering, and coherent scattering (see Fig. 1). The subtraction of each was accounted for in the statistical uncertainty except for that from coherent scattering in the cross section uncertainty (Fig. 3) because its correlation in the numerator and denominator of Eq. 3 was accounted for separately.

- i. The background due to pileup was corrected using the method of Ref. [18].
- ii. The radioactive room background was subtracted using a spectrum measured without beam.
- iii. The background due to small-angle Compton scattering originates from γ -rays first scattering at the collimators and then scattering on the inner wall of a Pb cylinder placed in the beam path between the collimator and the detectors. This process was simulated in Geant4 [19], and the simulation result was scaled to the spectrum and subtracted.
- iv. The background due to coherent atomic scattering was subtracted by first determining the coherent scattering cross section by fitting the directly measured beam profile [14], allowing only the area to vary, to the high-energy side of that part of the spectrum corresponding to elastically scattered γ -rays (see Fig. 1, bottom panel), where no contribution from NRF scattering was exhibited (0.28 ± 0.02 and 0.16 ± 0.04 mb at 2.28 and 2.75 MeV, respectively, were obtained, comparable with that expected from theory [20]), and then subtracting the cross-section normalized beam profile from the spectrum. Before fitting to the spectrum,

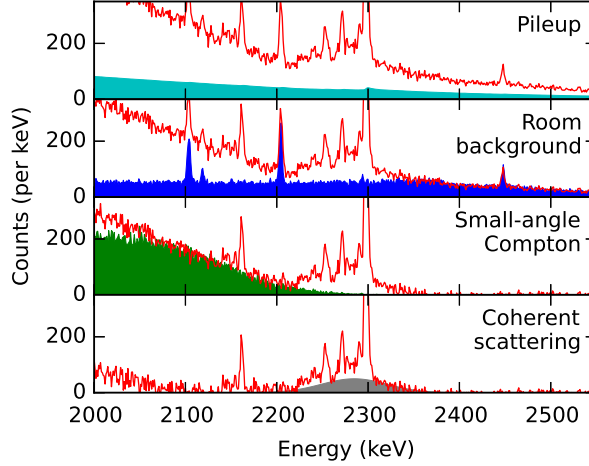


FIG. 1. (Color online) The background subtraction sequence in order of subtraction for the spectrum taken with no upstream absorber. The peaks at energy less than the beam energy (congruent with coherent scattering) are transitions to the excited state at 136 keV.

the beam profile was corrected for the energy dependency of the detector efficiency and coherent-scattering cross section (an inverse dependency with energy was assumed). The fitting and beam-profile uncertainties were accounted for in the subtraction.

Background from higher-energy NRF γ -rays interacting in the detectors but not resulting in full energy depositions was negligible (less than 3% effect), but was nevertheless subtracted using a Geant4 simulation.

From the background-subtracted NRF spectra, Fig. 2, the scattering strength, $b_i I_{cs}$, was determined for each peak from its area by using Eq. 1 in Ref. [14] and including a thick-target correction [12] (subscript i represents that some peaks may be transitions to excited states). The peak areas were determined in a least squares fit using a calibrated detector resolution. Peaks were added until the experimental spectrum was reproduced; more (or, less likely, fewer) peaks could be present. $\langle b_0 I_{cs} \rangle^*$ (Eq. 4) was then obtained for the set of peaks whose transition energies are in the region used to determine R (see below). To validate $\langle b_0 I_{cs} \rangle^*$, its value was also obtained using peak areas determined by summing the counts at each peak energy in appropriate intervals reflecting the peak spacing determined from fitting. The two $\langle b_0 I_{cs} \rangle^*$ values agreed within 2% at both energies. $\sigma_{\gamma\gamma}$ was also determined bin-by-bin by using the bin counts in the same equation for $b_0 I_{cs}$ weighted by the bin width [see Fig. 3]. The absorption ratio, R , was then obtained, by way of Eq. 3, from the average $\langle \sigma_{\gamma\gamma} \rangle$ for a specified energy region at each of the two beam energies (see absorption results below and Table I).

The NRF results confirm the large degree of fragmentation of dipole strength in odd-mass nuclei at both energies, adding 30 new peaks while verifying the 10 previously observed at these energies by Wolpert *et al.* [13] (see Fig. 2). At $E_\gamma = 2.28$ MeV, $2.8\times$ more strength in total (33 ± 4 eV b) was observed in small peaks than previously, going from 4 peaks to 15, not counting the large resonance (26 ± 1 eV b) at 2.298 MeV and its branch to the 136 keV state [21]. Three of the small peaks are branching transitions to the 136 keV state and were observed in the no absorber measurement only (see Fig. 1). Another three peaks may represent branching transitions to the 6 keV state and will be assumed as such for the sake of determining

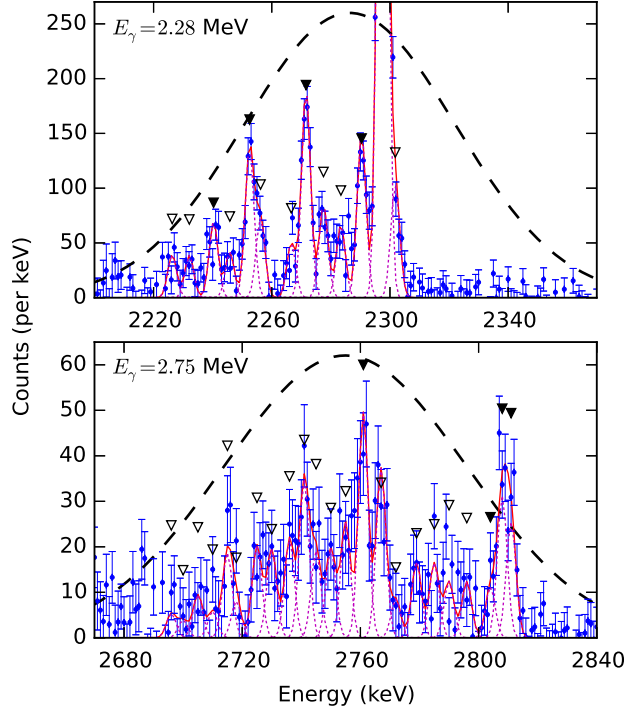


FIG. 2. (Color online) Background-subtracted spectrum for having no upstream absorber showing statistical uncertainty (blue points with error bars) and a fit to the NRF peaks (solid red line) with individual peaks displayed (dotted magenta lines). The beam profile is overlaid (dashed black line). Solid triangles mark previously observed transitions, and empty triangles mark newly observed transitions. Apparent peaks at the low-energy tail of the beam profile (below about 2.22 MeV and 2.70 MeV, top and bottom panel respectively) were not reproduced with an absorber in place, so they were not included in the fit. The peak of the 2.298 MeV resonance is at around 960 counts per keV.

average resonance properties. At $E_\gamma = 2.75$ MeV, $3.0\times$ more strength in total (28 ± 1 eV b) was observed than previous, going from 4 peaks to 23, with four of them possible branches to the 6 keV state.

The self-absorption results provide an extra dimension to the elastic-scattering results allowing the ground state branching ratio to be determined. At $E_\gamma = 2.28$ MeV in the region of weak transitions (2.230–2.293 MeV), significant absorption was observed that yielded $\langle I_{cs} \rangle^* = 12 \pm 3$ eV b (see Table I and Fig. 3). This is $4\times$ more than the average (weighted) elastic-scattering strength, $\langle b_0 I_{cs} \rangle^* = 2.9 \pm 0.3$ eV b (from Eq. 4) giving $\langle b_0 \rangle = 0.25^{+0.10}_{-0.06}$ by Eq. 5. Observed branching transitions can only account for another 12% of the total strength; the remaining 63% are branching transitions to states at higher energy than the first two excited states. The above $\langle b_0 \rangle$ value is close to the one that was calculated for all possible ground-state transitions from all possible spin states using a γ -ray cascade simulation for ^{181}Ta ($\langle b_0 \rangle \approx 0.4 - 0.5$) [22].

At $E_\gamma = 2.75$ MeV (2.722–2.814 MeV), moderate absorption was observed that yielded $\langle I_{cs} \rangle^* = 4 \pm 2$ eV b. This is $2\times$ more than $\langle b_0 I_{cs} \rangle^* = 1.8 \pm 0.1$ eV b giving $\langle b_0 \rangle = 0.5^{+0.7}_{-0.2}$.

The self-absorption results are validated in two ways using the data at $E_\gamma = 2.28$ MeV. First, the 2.298 MeV state's ground state branching ratio, b_0 , determined from $b_0 I_{cs}$ (elastic scattering) and I_{cs} (self-absorption) is smaller than but overlapping with b_0 determined assuming only the observed branch to the 136 keV state (see Table I). This holds true for both the Ta/None and the Ta/Pb absorber data sets. Second, the absorption ratios observed independently in the Ta/None and Ta/Pb absorber data sets are in

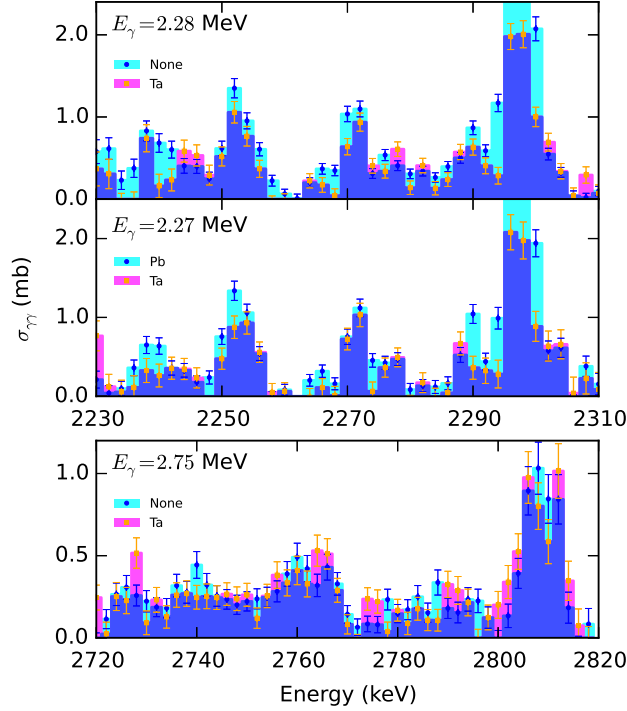


FIG. 3. (Color online) The elastic cross section, $\sigma_{\gamma\gamma}$, rebinned to 2 keV with statistical uncertainty. Cyan (blue circles) represents the no upstream absorber (or Pb absorber) spectrum. Magenta (orange squares) represents the Ta absorber spectrum. Resonant absorption (cyan above blue; blue indicates overlap of cyan and magenta) is evident at each beam energy.

TABLE I. The absorption properties for a region of small peaks at each of the two beam energies (2.230–2.293 MeV and 2.722–2.814 MeV) and for the single large peak. Uncertainties include both statistical and systematic sources added in quadrature. Rows 1 and 3 are averages of the $E_\gamma = 2.27$ and 2.28 MeV data sets.

E_γ MeV	$R(n_a)$	$\langle I_{cs} \rangle^*$ eV b	$\langle b_0 I_{cs} \rangle^*$ eV b	$\langle b_0 \rangle$
2.28	0.32 ± 0.07	12 ± 3	2.9 ± 0.3	$0.25^{+0.10}_{-0.06}$
2.75	0.14 ± 0.07	4 ± 2	1.8 ± 0.1	$0.5^{+0.7}_{-0.2}$
E_r	$R(n_a)$	I_{cs}	$b_0 I_{cs}$	b_0
2.298	0.64 ± 0.02	34 ± 2	26 ± 1	0.76 ± 0.06 0.83 ± 0.01^a

^a Branching ratio determined from observed transition to the 136 keV state.

agreement with each other for both the large peak at 2.298 MeV and the region of small peaks (see Fig. 3). The average of the two data sets is reported in Table I.

Combining the results from the NRF and self-absorption measurements indicate that a substantial portion of the scissors-mode strength has been observed here. Expected is about $\sum B(M1) \uparrow = 1.6 \mu_n^2$ (units of nuclear magnetons squared, see Ref. [2]), the same as that observed using NRF in neighboring ^{180}Hf and ^{182}W [23]. To compare, the scissors strength here was determined by weighting the summed elastic transition strength (converted to units of μ_n^2) with the ground state branching ratio and (since neither the spin nor the parity of the states could be determined) making the same assumptions made by Wolpert *et al.* [13] in their NRF measurement of ^{181}Ta : the same ratio of $M1$ to $E1$ strength as in the neighboring even-even nucleus

^{180}Hf (50%)—the measured strength here is a sum of the $M1$ and $E1$ strength—and a statistical spin factor of $g = 1$ for all states. A further assumption was made that the measured ground state branching ratio applies equally for $M1$ and $E1$ transitions. The present measurement then attributes to the scissors-mode $0.6 \pm 0.2 \mu_n^2$ (excluding the large resonance at 2.298 MeV), which is about 1/3 of the total expected strength of the scissors-mode. This amount is greater than the entire strength previously attributed to the scissors mode in ^{181}Ta (about $0.35 \mu_n^2$).

The present observation of increased strength could lead to resolving the discrepancy of the scissors-mode strength measured in the radiative decay and radiative excitation channels. The two present energies constitute only 1/10 of the previously investigated energy region or about 1/6 of the previously observed dipole strength (excluding the large resonance at 2.298 MeV). If the same pattern of increased strength, in the form of fragmentation and branching, were to hold across all energies, then significantly more scissors-mode strength, about $2\times$ that expected from systematics established using NRF, would be found in ^{181}Ta . This would be consistent with the expectations for enhanced scissors-mode strength from radiative decay experiments [6–9].

In conclusion, this Letter presented the first evidence of resonances at the energy of the scissors mode significantly branching ($\approx 75\%$) to excited states, while verifying the fragmentation of strength in odd-mass nuclei. The observation of branching invalidates a core assumption used to extract the total scissors-mode strength in odd-mass nuclei [5]. It, however, affirms the predictions for sizable coupling of the scissors mode to excited states [10], substantiates the expectations of large branching in ^{181}Ta from cascade simulations [22], and offers a route for resolving the discrepancy between the radiative decay and radiative excitation channels: branching, combined with fragmentation, may account for enough additional scissors-mode strength in the radiative excitation channel to match that observed in radiative decay. In such a case, theories of the scissors mode will need to be re-examined in order to understand the origin of the additional strength. Furthermore, significant branching of the scissors mode, if similarly found in odd-mass fissile isotopes, could lead to enhanced sensitivity in detection and assay applications using transmission NRF.

We would like to acknowledge the staff at the High Intensity γ -ray Source for providing excellent service and beams, M. Emamian for help with preparing the target holders, H. Karwowski and G. Rich for assistance during the experiment, and M. Omer for reviewing this paper. This study was supported by the Ministry of Education, Culture, Sports, Science and Technology (MEXT), Japan and by the National Nuclear Security Administration of the U.S. Department of Energy under Contract No. DE-AC02-05CH11231.

* angell.christopher@qst.go.jp

† National Institutes of Quantum and Radiological Science and Technology, Tokai-mura, Ibaraki 319-1106, Japan

[1] D. Bohle *et al.*, Phys. Lett. B **137**, 27 (1984).

[2] U. Kneissl, H. Pitz, and A. Zilges, Prog. Part. Nucl. Phys. **37**, 349 (1996).

[3] K. Heyde, P. von Neumann-Cosel, and A. Richter, Rev. Mod. Phys. **82**, 2365 (2010).

[4] N. L. Iudice and A. Richter, Phys. Lett. B **304**, 193 (1993).

- [5] J. Enders, N. Huxel, P. von Neumann-Cosel, and A. Richter, *Phys. Rev. Lett.* **79**, 2010 (1997).
- [6] M. Guttormsen *et al.*, *Phys. Rev. Lett.* **109**, 162503 (2012).
- [7] M. Krtićka *et al.*, *Phys. Rev. Lett.* **92**, 172501 (2004).
- [8] A. Schiller *et al.*, *Phys. Lett. B* **633**, 225 (2006).
- [9] A. Simon *et al.*, *Phys. Rev. C* **93**, 034303 (2016).
- [10] M. Harper and L. Zamick, *Phys. Rev. C* **91**, 054310 (2015).
- [11] W. Bertozzi *et al.*, *Phys. Rev. C* **78**, 041601(R) (2008).
- [12] B. Quiter *et al.*, *Nucl. Instrum. Meth. B* **269**, 1130 (2011).
- [13] A. Wolpert *et al.*, *Phys. Rev. C* **58**, 765 (1998).
- [14] C. Angell *et al.*, *Nucl. Instrum. Meth. B* **347**, 11 (2015).
- [15] F. Metzger, in *Progress in Nuclear Physics*, Vol. 7, edited by O. Frisch (Pergamon Press, New York, 1959) pp. 53–88.
- [16] The R defined in Ref. [14] is equivalent to $1-R$ given here. The present notation was adopted to be consistent with that given by Metzger [15].
- [17] H. Weller *et al.*, *Prog. Part. Nucl. Phys.* **62**, 257 (2009).
- [18] C. Angell, *J. Nucl. Sci. Tech.* **52**, 426 (2015).
- [19] S. Agostinelli *et al.*, *Nucl. Instrum. Meth. A* **506**, 250 (2003).
- [20] M. Schumacher, P. Rullhusen, F. Smend, and W. Mückenheim, *Nucl. Phys.* **A346**, 418 (1980).
- [21] The quoted NRF strength for 2.28 MeV through out is the average of the no absorber and Pb absorber measurements; there was a 22% average difference between them for small peaks and 7% difference between them for the 2.298 MeV resonance, the cause of which is unknown. The differences are reflected in the integrated cross section uncertainties. The absorption ratios, however, agreed between the respective sets.
- [22] A. Makinaga *et al.*, *Phys. Rev. C* **90**, 044301 (2014).
- [23] N. Pietralla *et al.*, *Nucl. Phys. A* **618**, 141 (1997).